PCCP

Accepted Manuscript

ROYAL SOCIETY OF CHEMISTRY

www.rsc.org/pccp

Journal Name

RSCPublishing

ARTICLE

Two-dimensional carbon-based materials with dynamically-controlled asymmetric Dirac cones

Cite this: DOI: 10.1039/xoxxoooooox

Received ooth January 2012,
Accepted ooth January 2012

DOI: 10.1039/xoxxoooooox

www.rsc.org/

Delia Miguel,[a] Irene R. Márquez,[a] Luis Álvarez de Cienfuegos,[a] Noelia Fuentes,[a] Salvador Rodríguez-Bolivar,[b] Diego J. Cárdenas,[c] Antonio J. Mota,*[d] Francisco Gómez-Campos*[b] and Juan M. Cuerva*[a]

The design of two dimensional graphene-type materials with an anisotropic electron flow direction in the X and Y axis opens the door to the development of novel electronic materials with multiple functions in nanoelectronics. In the present work, we have studied the electronic transport properties of a new family of 2D graphene-graphyne hybrid presenting conformationally free phenylethylene subunits. This system ensures two different conductive pathways perpendicular to each other: an acene nanoribbon subunit, in the X axis, with a graphene-type conduction, and a free to rotate phenylethylene subunit, in the Y-axis, in which the magnitude of the conduction depends dynamically on the corresponding torsion angle. Our calculations have confirmed that this system presents two different conduction pathways, which are related with the presence of asymmetric Dirac-type cones. Moreover, the Dirac cones can be dynamically modified in the presence of an external gate electrode, which is unprecedented in literature.

Introduction

Graphene has become a very promising two-dimensional (2D) carbon-based material for the near future development of molecular electronics owing to its unique properties derived from the presence of Dirac cones.[1,2] Recently it has been described that such Dirac cones are not exclusive of graphene, being present in other 2D materials such as graphyne family,[3-13] and janugraphene and chlorographene.[14] The reason seems to be the underlying graphene-type topology,[15] although exceptions have been described.[16] Interestingly, the Dirac-type cones in non-hexagonal situations[17] can be asymmetric in the X and Y axis, potentially allowing direction-dependent electron flow.[18] This remarkable asymmetry is observed in non-hexagonal systems as a result of the absence of hexagonal symmetry in the lattice. Nevertheless, although the slope of the cones can be tuned, it is determined by the structure of the material[19] and cannot be easily and reversibly modified in the presence of an external stimulus.[20] Within our recent interest in the design, synthesis, and evaluation of organic materials,[21] we thought that a new 2D graphene-graphyne hybrid based on simple acene[22] nanoribbons connected by conformationally flexible phenylethylene subunits could behave as a new dynamic 2D carbon-based material with interesting conductive properties.

In this work, we propose an anisotropic system, built by the minimum zigzag nanoribbon (acene nanoribbon) connected by alkynylphenyl-based molecular wires, in which, one conductive channel can be controlled by an external stimulus. The system has been also selected owing to the corresponding monomer and oligomers have already been experimentally obtained and future development of extended systems is expected.[23]

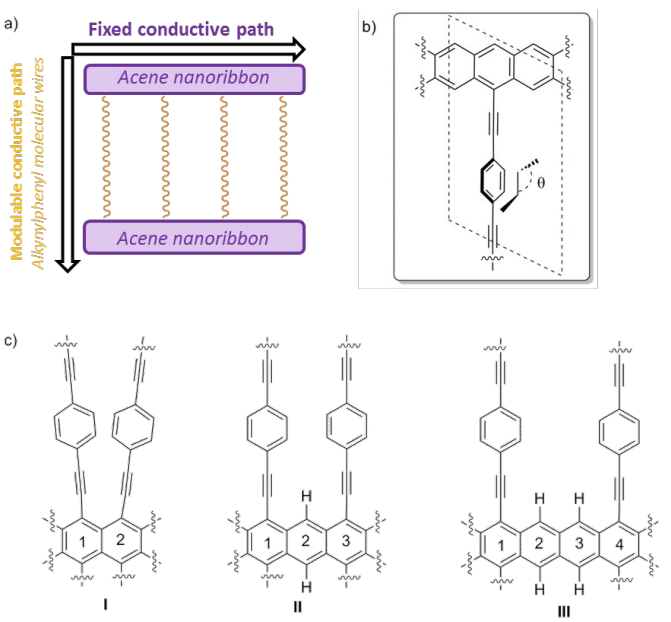

Fig.1. a) Schematic description of working hypothesis: 2D-systems composed by acene nanoribbons connected by alkynylphenyl-based molecular wires, b) θ angle definition, c) Examples of 2D cross-linked systems **I-III**.

This proposed material can be seen as composed by two different conductive pathways perpendicular each other. In the X axis, acene nanoribbon ensures a graphene-type Dirac-cone controlled conduction (Figure 1a). In the Y-axis phenylethylene subunits are also known to be molecular wires. Interestingly, the magnitude of the conduction is strictly correlated with the torsion angle θ of the mobile phenyl ring and the static acene nanoribbon (Figure 1b), showing a $\cos^2\theta$ dependence.[24,25] The experimental measurements of related systems have validated such dependence, and variations about two orders of magnitude in conductance have been observed. Therefore, the global 2D material would be anisotropic, presenting two main electronic pathways with different conductance. The control of the conductance through Y-pathway is therefore related with the control of torsion angle (θ). Considering the success of gated systems in the past, it would be desirable that an electric field could efficiently bias the conductance in the Y-axis, modifying the torsion angle by interaction with a dipolar moment in the mobile subunit.[26-28] With these premises we have found using SIESTA-based DFT calculations that despite the absence of hexagonal symmetry in the quasi 2D materials proposed in this work, they present asymmetric Dirac-type cones, which can be strongly modified in the presence of an external stimulus. A case of study using a gate electrode is also presented.

Results and discussion

Setting the system. The success of our system is based on the conformational freedom (possibility to turn) of the phenyl rings placed on the side chains of the acene nanoribbon and the control of such freedom using an external stimulus. To this end the interaction between the adjacent rotating aromatic rings must be carefully modulated. Moreover, the energy required for the interconversion between conformationally related structures must be low. That is, the orthogonal alkynylphenyl-based molecular wires must be easily placed close to the plane of the acene nanoribbon or perpendicular to that plane.

As we commented before, this is a key point because it is known that the conductivity through phenyl acetylenes and biphenyl systems is related to the angle (θ) (Figure 1b). Coplanar structures present low resistivity whilst perpendicular ones are much more insulating. On the other hand, the number of alkynylphenyl-based subsystems is also related to the intensity of the current in such direction and should be as high as possible. Taking into account the geometry of acene-based nanoribbons, such alkynylphenyl-based subsystems could be placed in [1,2]-, [1,3]-, [1,4]-, and so on, relative positions.[29] [1,2]-Consecutive positions (Figure 1c, **I**) resulted in such a tight packing that interaction between phenyl rings precludes rotation. [1,3]-Alternating positions (Figure 1c, **II**) allow the desired rotations with acceptable energies for the majority of the possible conformations. When we placed the side chains at [1,4]-relative positions (Figure 1c, **III**) the rotation is free but at the cost of use only one of the three possible conductive pathways. Therefore we selected **II** as basic structure for our study.

Substituents of benzene rings can also affect the conductance through them and also the dynamics of the system as a consequence of the steric hindrance. Moreover, other physical properties of the system, such as the dipolar moment, can be modified and can be subsequently used to control the system by an external electric field. In this work, we explored three possibilities using small hydrogen atoms (**IIa**), very bulky iodine atoms (**IIb**) and a mixed system (**IIc**) (Figure 2).

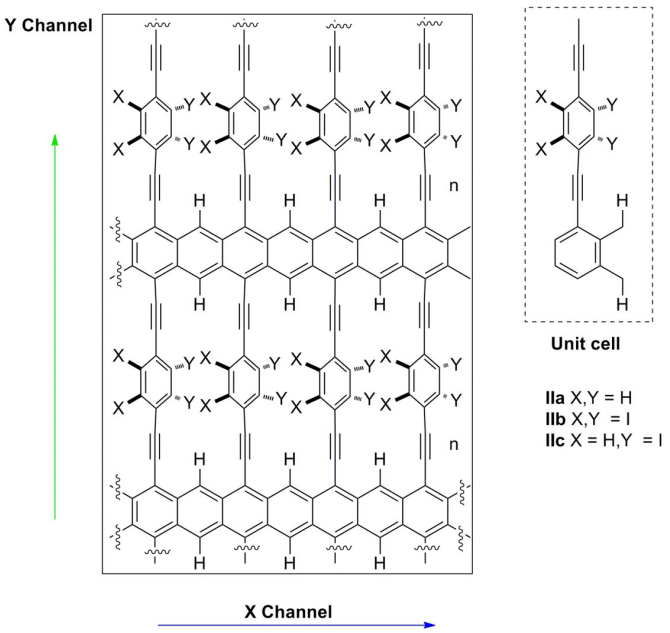

Fig. 2. a) Detailed structure of studied systems **IIa-c**, and b) unit cells of each system.

Potential energy surface of structures IIa-c. Beyond the simulation of the electronic behaviour of type-**II** static systems, we were mainly interested in the control of the rotation angle θ in these periodic systems in dynamic situations. In those cases, each phenyl ring is free to rotate, interacting with the other two spatially close phenyl rings. To accomplish this modelization, we carried out the study in simplified models **IVa-c** (Figure 3) by means of DFT calculations[30] carried out with the Gaussian 09 program,[31] employing the M05 hybrid functional developed by Truhlar and co-workers for a better description of long-range interactions.[32] All geometries were fully optimised by the gradient technique employing the following basis functions: for carbon and hydrogen the standard polarised 6-31G* basis set,[33] and for the iodine atom the SDD[34] large-core pseudo-potential was used with a supplementary *d* polarisation function (of exponent 0.266). The potential energy surface of those structures is θ dependent (Figure 3b) presenting a minimum which depends of the substitution of the rotating ring. For the less hindered one **IVa** the minimum is achieved for θ values around 40º. The inclusion of iodine atoms results in a dramatic change of the curve. The minimum energy of **IVb-c** is now at

θ values around 55º. Moreover, for lesser θ values the energetic cost for such rotation increases dramatically.

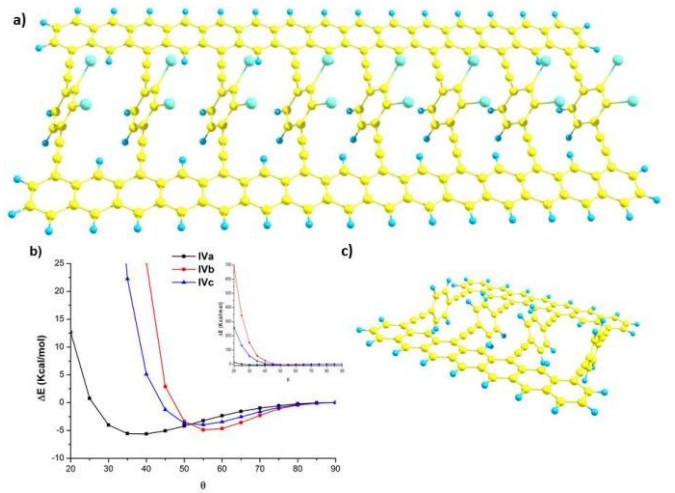

Fig. 3. a) Simplified models **IV** for structures **IIa-c**, exemplified with structure **IVc** with θ = 50º, b) Potential energy surface as function of θ angle for structures **IVa-c,** and c) Simplified model of **V** for structures **IIa-c**, exemplified with structure **Va** with θ = 50º

Nevertheless, in real systems each rotating aryl group could have a different θ angle value. To explore this complex situation we used model system **V** to study the relative energy of the inner aromatic rings in different relative configurations (θ_1 and θ_2) keeping the outer benzene rings at 90º. With such kind of calculations we could have a general idea of the behaviour of larger systems.

From the simulation of model **Va** (Fgure 4a), we could conclude that the system is very flexible and many combinations of torsional angles θ_1 and θ_2 are energetically accessible (0-6 kcal mol^{-1}) at room temperature (Figure 4). Thus for example, structures with θ_1:θ_2 values of 90:10, 70:20 and 50:40 presented almost the same energy. The only exception is the presence of two consecutive planar or quasi-planar dispositions (θ_1 and θ_2 values simultaneously below 20º). Therefore, at room temperature a completely disordered material is expected, presenting consecutive low θ angle highly conductive structures and high θ angle insulating ones.

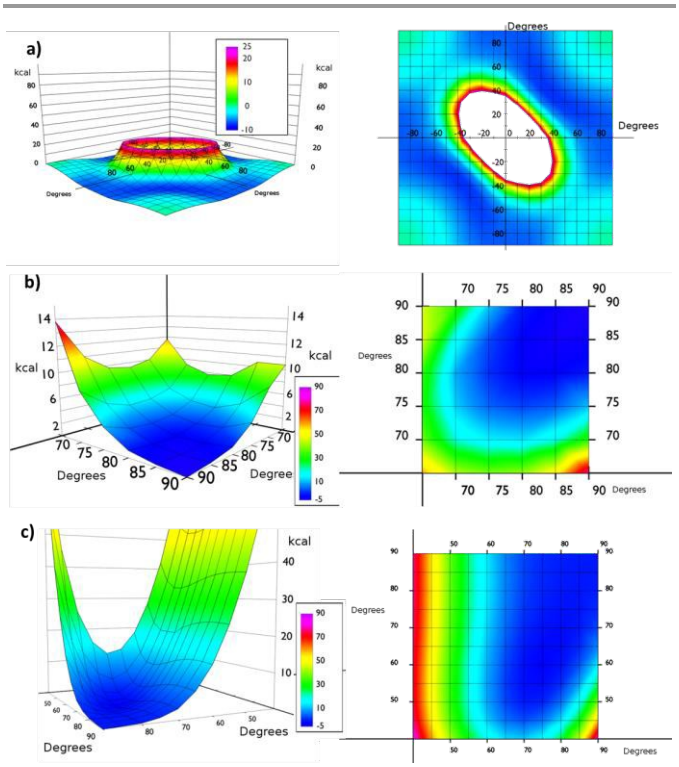

Fig. 4. Top and side views of potential energy surface of systems a) **Va**, b) **Vb**, and c) **Vc**.

The presence of bulkier iodine atoms strongly restricts the freedom of the system. In **Vb** the most favourable situation is when θ_1:θ_2 values are 90º, being θ angles below 45º energetically unavoidable at room temperature (Figure 4b). This fact derives from the overlap of iodine atoms during the rotation movement. This result also suggests that a correlation of the individual movement of the aromatic ring in the material might exist. The artificial restriction of only one phenyl ring might trigger a domino effect over the rest of the phenyl rings in the same row, thus helping in the orientation of the system using shear stress. An inspection of the potential energy surface of **Vb** showed that if θ_1 value up to 80º the minimum energy of the system is allowed for the same θ_2. This fact suggests that some ordering can be imposed in the global system applying a shear stress in isolated part of it, thus resembling the operation of a Venetian blind. With θ_1 values below 80º the correlation is partially lost and long range effects are more difficult to analyze.

We also studied the asymmetrically substituted structure **Vc**. In this case the configuration of minimum energy (1.36 kcal mol^{-1}) corresponds to θ_1 and θ_2 values of 75º and 65º respectively. Again, angles below 45º are energetically unavoidable at room temperature. In any case, in the potential energy surface a correlation motion can be observed for high θ_1 values (80º).

Electronic properties of structures type-II

Structure IIa. The simulation of the band structure of disordered material **IIa** is complex owing to the number of potential structures depending on the θ angle of each phenyl ring in the continuous material. The study could be simplified if the global conductivity in the Y axis were considered as a simple summation of each individual θ-dependent molecular wire. If this situation were operative we should observe similar band structures for systems **II** and **III** (Figure 1c) in which the overlapping between the consecutive phenyl rings is completely different. Fortunately, when we simulated such band structures we found closely related features for all the θ angles. These results suggest that the conduction through the rotated phenyl rings (y-direction) is more or less independent on the inter-phenyl interactions. Thus, the global conduction in our model structure **IIa** can be seen as a summation of the contribution of each individual pathway. Therefore, we simulated the band structure of **IIa** with all the free to rotate phenyl rings frozen at selected θ angles from 0 to 90º using SIESTA package.[35]

The reciprocal space of **IIa** is two dimensional, since it periodically extends along the acene nanoribbon (x-axis) structure and perpendicular to them (y-axis). The angle of the phenyl group does not affect the dimensions of the Brillouin zone. Thus, it is possible to analyze the effects of conformational changes using the same range of k_x and k_y. We sampled the first Brillouin zone to obtain the 3D band structure showed in Figure 5. Calculations were carried out placing the Fermi energy level as the reference of energies, i. e. E_F =0. A clearer view of the studied phenomena can be seen in the corresponding top and bottom views of the corresponding valence and conduction bands (Figure 5) Regarding **IIa**, we rotated the phenyl groups from 10º to 90º in steps of 10 degrees.

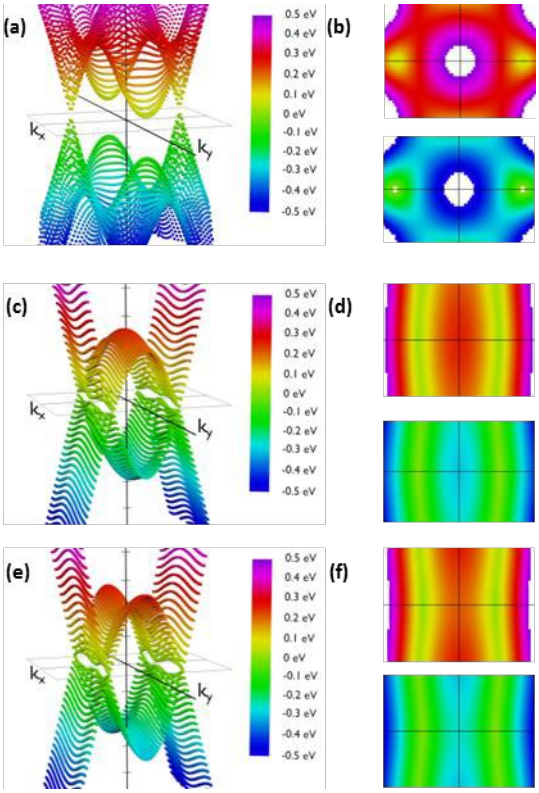

Fig. 5. Energy dispersion relations for structure **IIa** for orientations θ = 20º (a and b), θ = 70º (c and d) and θ = 90º (e and f). Figures (a), (c) and (e) are energy vs k_x and k_y from a side view. Figures (b), (d) and (f) are the same figures from the top (reddish representations) and from the bottom (bluish representations). Figures (a) and (b) show a well defined couple of Dirac cones and two parabolic extrema along the perpendicular direction; (c), (d), (e) and (f) show the evolution to a folding in the band along the k_y direction. The slope along the k_y direction keeps being stepped while it decreases along the k_x direction when the angle increases for both the Dirac cones and the parabolic extrema. Further, the parabolic extrema and Dirac cones align themselves creating the folding.

We observed that low θ angles (10º-50º) reveal two well defined Dirac cones placed on the k_x axis. Apart from these, on the k_y axis in the Brillouin zone boundary there are parabolic extrema. Conduction and valence bands have these parabolic extrema at the same positions in the reciprocal space. A vertical band gap is observed between these parabolic relative extrema. As an example its width is 141 meV for a 20 degrees rotation configuration. When the angle is increased the Dirac cones move along the k_x axis slightly approaching the gamma point. At the same time the cones slopes significantly decrease along the k_y axis. In this manner, the Dirac cones and the extrema in the Brillouin zone boundary create a fold along the k_y axis having a parabolic profile along that direction.

Remarkably, the cones are not symmetric due to the different slopes of the bands in each direction. As a consequence, dissimilar slopes have been obtained in different directions. We are especially interested in the variation of the slopes from the k_x to the k_y directions, since the k_x direction would correspond to current along the acene nanoribbons whilst k_y direction would correspond to current along the dynamic connections, which are influenced by the θ angle. The anisotropic

conductivity of the samples is affected by these slopes since the slope is proportional to the group velocity of electrons along each direction. The corresponding group velocity can be obtained from the computed slopes by dividing them by ħ.

As expected, the shape of the band structure is dramatically dependent of the θ angle and these slope asymmetries increase dramatically when increasing the angle. For angles between 50º and 60º the extrema in the Brillouin zone boundaries are clearly split off. In addition, the Dirac cones reduce drastically the slope along the Y axis. The result of this flattening is to connect the extrema in the boundaries with the region of the initial Dirac cones, transforming the cones into folds. This structure is kept almost unmodified for angles up to 90º. This change is crucial to understand how the system would behave under the application of an external voltage along the Y direction, suggesting that conduction would be considerably different along the X and the Y directions for configurations with high angles due to the dramatic change in the electron group velocity. On the other hand, comparable conductions for low angles would be detected. Further, the band structure suggests that this modification is not gradual, but it changes dramatically from 50º to 70º. Therefore, pushing the phenyl rings closer to the acene nanoribbon plane may result in conduction through the phenyls. Rotating them more than 70º respect to that plane would decouple the π-based molecular orbitals of the phenyl ring and the acene nanoribons, giving rise to a clearly anisotropic conduction, specially reduced through the phenyl-based pathways.

In order to quantify the observed features in the Structure **IIa** we calculated the slopes along different directions in the Brillouin zone. Figure 6 shows the absolute values of the slopes about the extrema for the conduction and valence band respectively. The referred to as "first cone" in the figures is the described Dirac cone placed on the k_X axis, and the referred to as "second cone" in the figures stands for the extrema in the Brillouin zone boundaries. The studied cones were placed in the region $k_x>0$ and $k_y>0$. The direction $+k_x$ in each case is the one going further from the gamma point, and the opposite for the $-k_x$. Regarding the Y direction, $+k_y$ and $-k_y$ directions where also studied. These were found to be exactly symmetrical in all the cases.

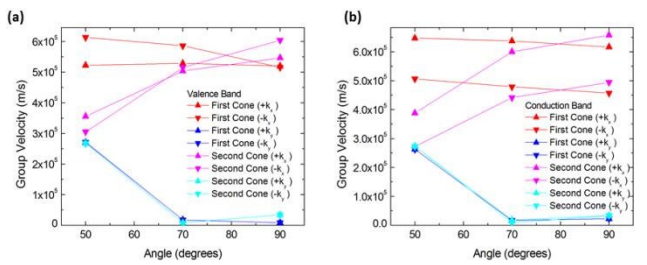

Fig. 6. Group velocities in (a) valence and (b) conduction bands vs θ angles for structure **IIa**. Red and blue data correspond to the first cones (those fully included in the Brillouin zone) while pink and cyan correspond to the second cones (those in the Brillouin zone boundaries). Red and pink data are for group velocities along the k_x direction, blue and cyan data correspond to k_y direction. Group velocities along the k_y direction noticeably decrease for increasing angles.

The figurealso shows that the slopes along the k_X directions where almost constant for the first cone in the interval from 50º to 90º, and they increase for the second cones in the same interval. The slopes along the k_X direction for both extrema and both bands (conduction and valence) are of the same order of magnitude. The most interesting feature of these figures is the great drop in the slope from 50º to 70º in conduction and valence bands. To correctly interpret these details it is necessary to mention that the right meaning of them is a rapid modification in the band profile from a cone to a fold taking place in this narrow angle interval. Therefore conduction along the y direction should not be quantified by means of the slope for high angles, but using an effective mass instead. Nevertheless, the effective masses are large and as a consequence the conductance would be small. For instance, at 90º the electron effective mass in the conduction band along the Y direction and about the first cone is $m\approx37m_0$. Thus, under these conditions the contribution of conduction along the y direction is negligible.

Structure IIb. Simulation of more angle-constrained material **IIb** was carried out in the same way. Taking into account the potential energy profile previously obtained we only simulated the band structure for structures with θ values from 50º to 90º (Figure 7). Similar features related to the above presented system were observed, especially regarding to the dramatic modification from almost isotropic to anisotropic conductivity in a short angle interval. In this case we could again observe the transition around 70º.

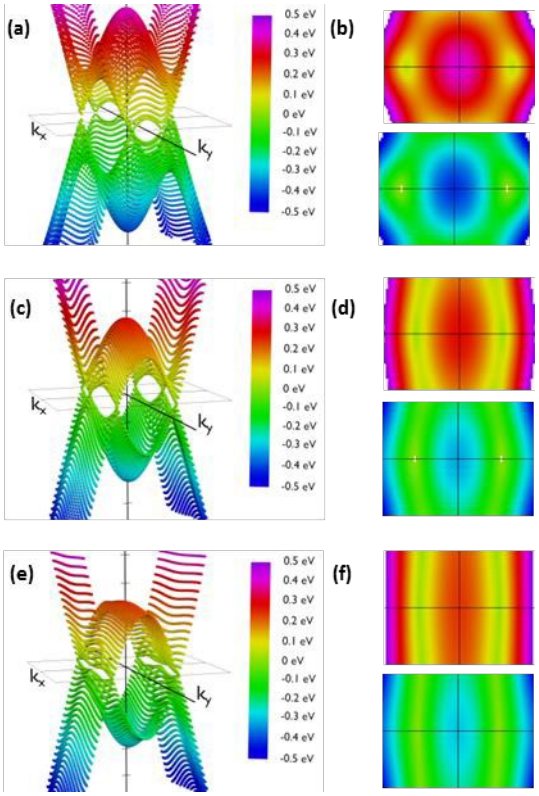

Fig. 7. Energy dispersion relations for structure **IIc** for orientations θ = 50º (a and b), θ = 70º (c and d) and θ = 90º (e and f). Figures (a), (c) and (e) are energy vs k_x and k_y from a side view. Figures (b), (d) and (f) are the same figures from the top (reddish representations) and from the bottom (bluish representations). Figures (a) and (b) are a copule of Dirac cones and other similar structures close to the Brillouin zone boundaries; (c), (d), (e) and (f) show the evolution to a folding in the band along the k_y direction. The slope along the k_y direction keeps being stepped while it decreases along the k_x direction when the angle increases for both Dirac cones. Further, the parabolic extrema and Dirac cones align themselves creating the folding.

Calculated slopes for the representative cones for conduction and valence bands at different angles are also illustrative (Figure 8). Many common features can be noticed. Firstly, the order of magnitude of slopes is the same than for **IIa**. The behaviour of the slopes along the k_x and $k_y$directions also reminds structure **IIa**. The drops in the curves for slopes along the k_y direction seem to be more gradual, but still dramatic. The right interpretation of the slopes for angles above 70º is again a transformation of the cones into parabolas. As a result, this structure would also behave anisotropically regarding electron transport for angles greater than a critical angle (about 80º), being the conduction controlled by the acene subsystem. Below such critical angle, conduction in both x and y directions is possible.

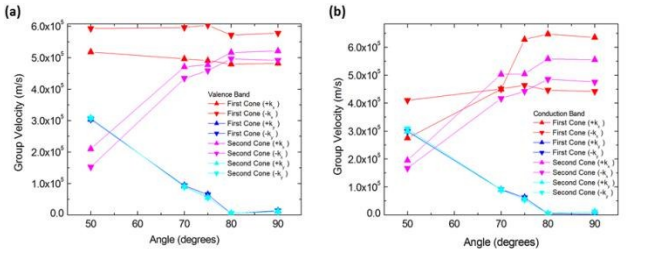

Fig. 8. Group velocities in (a) valence and (b) conduction bands vs θ angles for structure **IIb.** Red and blue data correspond to the first cones (those fully included in the Brillouin zone) while pink and cyan correspond to the second cones (those in the Brillouin zone boundaries). Red and pink data are for group velocities along the kx direction, blue and cyan data correspond to ky direction. Group velocities along the kydirection noticeably decrease for increasing angles.

Structure IIc. Band structure of material **IIc** is essentially identical to those described for **IIb** (Figure 9). In this case, we simulated again the band structure for structures with θ values from 50º to 90º, finding the transition around 80º (Figure 10).

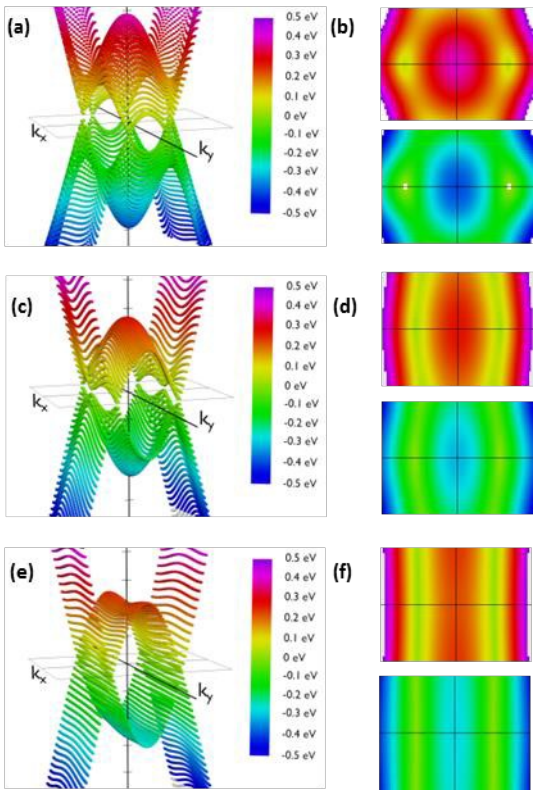

Fig. 9. Energy dispersion relations for structure **IIc** for orientations θ = 50º (a and b), θ = 70º (c and d) and θ = 90º (e and f). Figures (a), (c) and (e) are energy vs k_x and k_y from a side view. Figures (b), (d) and (f) are the same figures from the top (reddish representations) and from the bottom (bluish representations). Figures (a) and (b) are a copule of Dirac cones and other similar structures close to the Brillouin zone boundaries; (c), (d), (e) and (f) show the evolution to a folding in the band along the k_y direction. The slope along the k_y direction keeps being stepped while it decreases along the k_x direction when the angle increases for both Dirac cones. Further, the parabolic extrema and Dirac cones align themselves creating the folding.

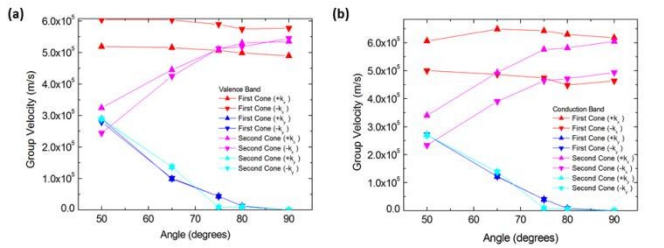

Fig. 10. Group velocities in (a) valence and (b) conduction bands vs θ angles for structure **IIc**. Red and blue data correspond to the first cones (those fully included in the Brillouin zone) while pink and cyan correspond to the second cones (those in the Brillouin zone boundaries). Red and pink data are for group velocities along the k_x direction, blue and cyan data correspond to k_y direction. Group velocities along the k_y direction noticeably decrease for increasing angles.

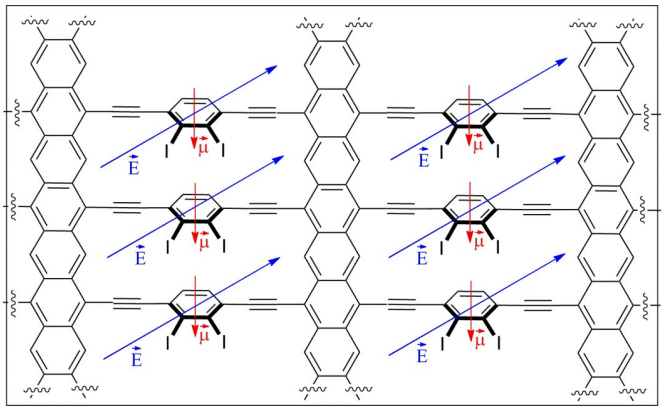

Fig. 11. Proposed effect of an electric field on structure **IIc** possessing a dipolar moment.

Control of θ angle distribution intype-II structures.

In absence of any ordering stimulus, the global conduction along the Y direction in structures type-**II** would be a superposition of contributions of each angular configuration weighted by its corresponding probability of occurrence, which can be estimated from Boltzmann statistics. Taking into account that in all the cases the energetically favoured θ values are around 35-60º, the transport properties would be dominated by conductive pathways. In any case, the small potential energy differences (up to 7 kcal mol^{-1}) between such optimum angle and 90º suggest that at room temperature an important number of channels would be operating under other less conductive regimen. Moreover each individual channel would be also jumping from one state to another.

Bearing these ideas in mind, the main goal would be the control over global distribution of rotating phenyl rings, which is the ultimate responsible of the anisotropic properties of the material. An external stimulus must be responsible to surpass the energetic penalty associated with such control, especially at room temperature. For disordered material **IIa** the desired control is not a simple task. For that reason we focussed our attention in more angle-constrained materials **IIb** and **IIc**. Between them, the presence of a permanent dipolar moment in the rotating phenyl group present in **IIc** could serve to induce the desired order. The presence of an electric field (gate electrode) perpendicular to the structure (Z axis) should induce a torsional force able to distort the original Boltzmann equilibrium distribution in absence of the electric field. Depending on the magnitude of the dipolar moment and the magnitude and sign of the electric field, different Boltzmann distribution could be obtained. For simplicity the Boltzmann distribution was constructed from an ideal system in which all θ angles have the same value (Figure 3a), including high energy states up to 686 kcal mol^{-1}.

We then simulated the Boltzman distribution of structure **IIc** in the presence of an electric field. First, we calculated the dipolar moment of the rotating substructure, yielding a value of 2.2 Dby, which is similar to that observed in related systems. The energy of the interaction of such dipolar moment in an electric field was added to the energy of the θ population at room temperature. The results are summarized in the following Figure 12.

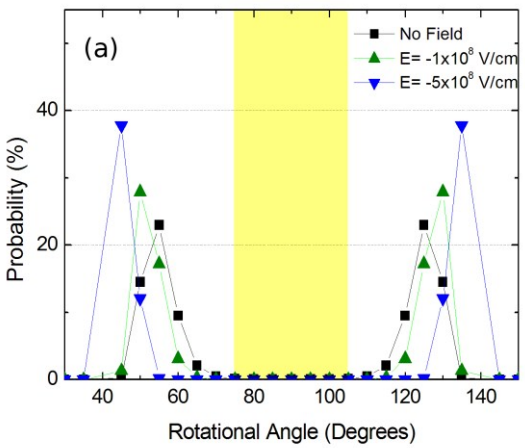

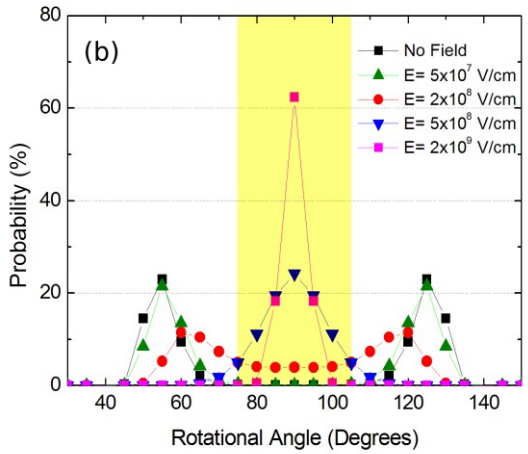

Fig. 12. a) negative electric fields, and b) positive electric fields. Light brown areas represent Y-insulating θ angle values Calculations were carried out at 300K.

The figure shows that angles about 50º (and likewise 130º) are the most likely to occur under no electric field. As it can be also seen the presence of the electric field is able to dramatically change the distribution profile, allowing a completely ordered material with homogeneous conductive or not conductive pathways in the Y direction. In the second case is remarkable that the switch from a conductive to an insulating material would be reversible just applying or not the electric field. In the described case the required electric fields are comparable with those found in other devices, such as short channel MOSFETs. In any case, this electric field values can be diminished increasing the value of the dipolar moment, that is, changing the substituent and/or the shape and size of the rotating system.

Computational methods

Modelling of conformational flexibility of structures type-II. Geometry optimization of model systems **IV** and **V** and the corresponding θ variation calculations was carried out at the DFT level of theory (see above).

Modelling band structure of type-II structures. From previous optimized structures **IV** and **V** we built a sheet. The geometry of the supercell was then fully optimized at DFT level with Perdew-Burke-Ernzerhof generalized-gradient approximation (GGA-PBE) functional[36] with a double-ζ plus polarization basis set until forces acting in each atom is less than 0.02 eV/Å using the Spanish Initiative for Electronic Simulations with Thousands of Atoms (SIESTA 2.0.2) code.[35] During that relaxation the studied angle θ is fixed. A vacuum layer of 20 Å was also chosen to prevent interaction between adjacent sheets. We also selected a 5 mRy energy-shift parameter, and a 11×11 Monkhorst-Pack grid for electronic structure calculations, which ensured convergent results for all the calculations. Test calculations with larger basis set and mesh cut-off were also performed, which gived almost identical results. During these calculations, core electrons and nuclei are replaced by Troullier-Martin's norm-conserving pseudopotentials.[37]

Modeling Boltzmann distribution. The system has been modelled as a set of non-interacting phenyl rings, each one with a particular angular orientation which energy is known from the theoretical calculations above presented. From it we calculated the probability of each angular orientation as follows:

$$P(\theta) = \frac{e^{-\epsilon_\theta / k_B T}}{\sum_\theta e^{-\epsilon_\theta / k_B T}}$$

θ being the phenyl ring, k_B being the Boltzmann´s constant and T the temperature of the system. We sampled the configurations in angles from 20º to 160º in steps of 5º in order to numerically calculate the probabilities.

In order to calculate the probability of each configuration under the application of an external electric field, the energy of the system was modified to include that effect. In this manner, the energy of a particular angular orientation is the following:

$$\epsilon_\theta = \epsilon_{\theta,nofield} - \vec{\mu} \cdot \vec{E}$$

These values were used to calculate the new energies and were included in the above equations to obtain the new probabilities.

Conclusions

In summary, we have designed and theoretically studied a family of 2D graphene-graphyne hybrid type materials with two different conductions pathways that can be externally modified with an electric field. The influence of θ angles values in the potential energy surface of type-**II** structures was calculated. Next, the influence of the θ values in the electronic properties was studied. As expected, the shape of the band structure was dependent of the θ angle. At low θ angles (10º-50º) the structures presented well defined Dirac cones on the k_X axis while at high θ values the Dirac cones reduced drastically the slope along the k_Y axis. This suggests that at higher θ values the conduction along the X and the Y directions must be different. Finally, we have shown that a gate electrode in structures presenting a dipolar moment (**IIc**) can modulate the global distribution of the rotating phenyl rings, thus allowing a new type of 2D material in which their electronic properties could be dynamically controlled. Therefore, these proposed 2D-materials are essentially a promising 2D switch. Partial and controlled switching of localized areas of this extended material could be also used for information storage or logic calculations.

Acknowledgements

We thank the MICINN (project CTQ-2011.22455) and theRegional Government of Andalucía (project P09-FQM-04571) for financial support, the 'Centro de Supercomputación de la Universidad de Granada (UGRGRID-CSIRC)' for computation time. NF and DM thank MICINN for their research contracts.

Notes and references

[a] Department of Organic Chemistry, Faculty of Science, University of Granada, Granada (Spain); E-mail: jmcuerva@ugr.es.

[b] Department of Electronic and Computer Technology, Faculty of Science, University of Granada, Granada (Spain). E-mail: fmgomez@ugr.es

[c] Department of Organic Chemistry, Universidad Autónoma de Madrid, Madrid (Spain).

[d] Inorganic Chemistry, Faculty of Science, University of Granada, Granada (Spain). E-mail: amota@ugr.es

References

1 C. N. R. Rao, H. S. S. R. Matte, K. S. Subrahmanyan, *Acc. Chem. Res.* 2013, **46**, 149-159.

2 A. C. Ferrari, F. Bonaccorso, V. Fal'ko, K. S. Novoselov, S. Roche, P. Bøggild, S. Borini, F. H. L. Koppens, V. Palermo, N. Pugno, J.A. Garrido, R. Sordan, A. Bianco, L. Ballerini, M. Prato, E. Lidorikis, J. Kivioja, C. Marinelli, T. Ryhänen, A. Morpurgo, J. N. Coleman, V. Nicolosi, L. Colombo, A. Fert, M. Garcia-Hernandez, A. Bachtold, G. F. Schneider, F. Guinea, C. Dekker, M. Barbone, Z. Sun, C. Galiotis, A. N. Grigorenko, G. Konstantatos, A. Kis, M. Katsnelson, L. Vandersypen, A. Loiseau, V. Morandi, D. Neumaier, E. Treossi, V. Pellegrini, M. Polini, A. Tredicucci, G. M. Williams, B. H. Hong, J.-H. Ahn, J. M. Kim, H. Zirath, B. J. van Wees, H. van der Zant, L. Occhipinti, A. Di Matteo, I. A. Kinloch, T. Seyller, E. Quesnel, X. Feng, K. Teo, N. Rupesinghe, P. Hakonen, S. R. T. Neil, Q. Tannock, T. Löfwander, J, Kinaret, *Nanoscale*, 2015, **7**, 4598-4810.

3 R. H. Baughman, H. Eckhardt, M. Kertesz, *J. Chem. Phys.* 1987, **87**, 6687-6699.

4 A. N. Enyashin, A. I. Ivanoskii, *Phys. Status Solidi B* 2011, **248**, 1879-1883.

5 Y. Li, L. Xu, H. Liu, Y. Li, *Chem. Soc. Rev.* 2014, **43**, 2572.

6 A. L. Ivanovski, *Progress in sol. St. Chem.* 2013, **41**, 1-19.

7 D. Malko, C. Neiss, F. Viñes, A. Görling, *Phys. Rev. Lett.*2012, **108**, 086804.

8 B. G. Kim, H. Choi, *Phys. Rev. B*, 2012, **86**, 115435.

9 X. Niu, X. Mao, D. Yang, Z. Zhang, M. Si, D.Xue, *Nanoscale Res. Lett.* 2013, **8**, 469.

10 L.-C. Xu, R.-Z. Wang, M.-S. Miao, X.-L. Wei, Y.-P. Chen, H. Yan, W.-M. Lau, L.-M. Liu, Y.-M. Ma, *Nanoscale*, 2014, **6**, 1113.

11 A. Wang, L. Li, X. Wang, H. Bu, M. Zhao, *Diamond & related materials* 2014, **41**, 65-72.

12 O. Leenaerts, B.Partoens, F. M. Peeters, *Appl. Phys. Chem.* 2013, **103**, 013105.

13 D. Malko, C. Neiss, A. Görling, *Phys. Rev. B*, 2012, **86**, 045443.

14 Y. Ma, Y. Dai, B. Huang, *J. Phys. Chem. Lett.* 2013, **4**, 2471-2476.

15 H. Huang, W. Duan, Z. Liu, *New J. Phys.* 2013, **15**, 023004.

16 L.-C. Xu, R.-Z. Wang, M.-S. Miao, X.-L. Wei, Y.-P. Chen, H. Yan, W.-M Lau, L.-M Liu, Y.-M. Ma, *Nanoscale* 2014, **6**, 113-118.

17 J. Wang, H. Huang, W. Duan, Z. Liu, *J. Chem. Phys.* 2013, **139**, 184701.

18 X. Lin, H.-L- Wang, H. Pan, H.-Z. Xu, *Chin. Phys. Lett.*2013, **30**, 077305.

19 J. Peng, Z.-G. Fu, S.-S. Li, *Appl. Phys. Lett.*2012, **101**, 222108.

20 H.-J. Cui, X.-L. Sheng, Q.-B. Yan, Q.-R. Zheng, G. Su, *Phys. Chem. Chem. Phys*. 2013, **15**, 8179-8185.

21 (a) N.Fuentes, A.Martín-Lasanta, L. Álvarez de Cienfuegos, R. Robles, D. Choquesillo-Lazarte, J. M. García-Ruiz, A. J. Mota, L. Martínez-Fernández, I. Corral, D. J. Cárdenas, M. Ribagorda, M. C. Carreño, J. M. Cuerva, *Angew. Chem., Int. Ed*. 2012, **51**, 13036-13040; (b) A. Martin-Lasanta, L. Álvarez de Cienfuegos, A. Johnson, D. Miguel, A. J. Mota, Á. Orte, M. J. Ruedas-Rama, M. Ribagorda, D. J. Cárdenas, M. C. Carreño, A. M. Echavarren, J. M.Cuerva, *Chem. Sci*. 2014, **5**, 4582-4591. (c) D. Miguel, S. P. Morcillo, A. Martín-Lasanta, N. Fuentes, L. Martínez-Fernández, I. Corral, M. J. Ruedas-Rama, D. J. Cárdenas, L. Álvarez de Cienfuegos, Á. Orte, J. M. Cuerva *Org. Lett.* 2015, **17**, 2844-2847. (d) S. Rodríguez-Bolívar, F. M. Gómez-Campos, L. Álvarez de Cienfuegos, N. Fuentes, D. J. Cárdenas, E. Buñuel, J. E. Carceller, A. Parra, J. M. Cuerva, *Phys. Rev. B*, 2011, **83**, 125424 (e) N. Fuentes, A. Martín-Lasanta, L. Álvarez de Cienfuegos, M. Ribagorda, A. Parra, J. M. Cuerva, *Nanoscale*, 2011, **3**, 4003 (f) A. J. Mota, L. Álvarez de Cienfuegos, S. P. Morcillo, N. Fuentes, D. Miguel, S. Rodríguez-Bolívar, F. M. Gómez-Campos, D. J. Cárdenas, J. M. Cuerva, *ChemPhysChem* 2012, **13**, 3857 (g); A. Martín-Lasanta, D. Miguel, T. García, J. A. López-Villanueva, S. Rodríguez-Bolivar, F. M. Gómez-Campos, E. Buñuel, D. J. Cárdenas, L. Álvarez de Cienfuegos, J. M. Cuerva, *ChemPhysChem*, 2012, **13**, 860.

22 M. Watanabe, K.-Y. Chen, Y. J. Chang, T. J. Chow, *Acc. Chem. Res.* 2013, **46**, 1606-1615.

23 M. M. Rauhut, B. G. Roberts, D. R. Maulding, W. Bergmark, R. Coleman, *J. Org. Chem.* 1975, **40**, 330-335.

24 A. Mishchenko, D. Vonlanthen, V. Meded, M. Burkle, C. Li, I. V. Pobelov, A. Bagrets, J. K. Viljas, F. Pauly, F. Evers, M. Mayor, T. Wandlowski, *Nanolett.* 2010, **10**, 156-163.

25 A. Mishchenko, L. A. Zotti, D. Vonlanthen, M. Burkle, F. Pauly, J. C. Cuevas, M. Mayor, T. Wandlowski, *J. Am. Chem. Soc.* 2011, **133**, 184-187.

26 H. Wan, B. Zhou, X. Chen, Q. S. Sun, G. Zhou, *J. Chem. Phys. C* 2012, **116**, 2570-2574.

27 L.-Y. Hsu, E. Y. Li, H. Rabitz, *Nanolett.*2013,**13**, 5020-5025.

28 L.-Y. Hsu, C.-Y. Chen, E. Y. Li, H. Rabitz, *J. Chem. Phys. C* 2015, **119**, 4573-4579.

29 A related structure without the phenyl groups was described as a semiconductor with a very low band gap: A. N. Enyashin, A. I.Ivanoskii, *Phys. Status Solidi B* 2011, **248**, 1879-1883.

30 A. D. Becke, *Phys. Rev. A*1988, **38**, 3098−3100.

31 M. J. Frisch, G. W. Trucks, H. B. Schlegel, G. E. Scuseria, M. A. Robb, J. R. Cheeseman, G. Scalmani, V. Barone, B. Mennucci, G. A. Petersson, H. Nakatsuji, M. Caricato, X. Li, H. P. Hratchian, F. Izmaylov, J. Bloino, G. Zheng, J. L. Sonnenberg, M. Hada, M. Ehara, K. Toyota, R. Fukuda, J. Hasegawa, M. Ishida, T. Nakajima, Y. Honda, O. Kitao, H. Nakai, T. Vreven, J. A. Montgomery, Jr., J. E.

Peralta, F. Ogliaro, M. Bearpark, J. J. Heyd, E. Brothers, K. N. Kudin, V. N. Staroverov, T. Keith, R. Kobayashi, J. Normand, K. Raghavachari, A. Rendell, J. C. Burant, S. S. Iyengar, J. Tomasi, M. Cossi, N. Rega, J. M. Millam, M. Klene, J. E. Knox, J. B. Cross, V. Bakken, C. Adamo, J. Jaramillo, R. Gomperts, R. E. Stratmann, O. Yazyev, A. J. Austin, R. Cammi, C. Pomelli, J. W. Ochterski, R. L. Martin, K. Morokuma, V. G. Zakrzewski, G. A. Voth, P. Salvador, J. J. Dannenberg, S. Dapprich, A. D. Daniels, O. Farkas, J. B. Foresman, J. V. Ortiz, J. Cioslowski and D. J. Fox, *Gaussian 09, Revision B.01*; Gaussian, Inc.: Wallingford CT, 2010.

32 (a) Y. Zhao, N. E. Schultz, D. G. Truhlar, *J. Chem. Phys.* 2005, **123**, 161103. (b) Y. Zhao, D.G. Truhlar, *Acc. Chem. Res.* 2008**, 41**, 157.

33 W. Kuelche, M. Dolg, H. Stoll, H. Preuss, *Mol. Phys.* **1991**, *74*, 1245.

34 W. J. Hehre, R. Ditchfield, J.A. Pople, *J. Chem. Phys.***1972,** *56*, 2257.

35 J. M. Soler, E. Artacho, J. D. Gale, A. Garcia, J. Junquera, P. Ordejon, D. Sanchez-Portal, *J. Phys.: Condens. Matt.* 2002, **14**, 2745.

36 J. P. Perdew, K. Burke, M. Ernzerhof, *Phys. Rev. Lett.* 1996, **77**, 3865.

37 N. Troullier, J. L. Martins, *Solid State Commun.* 1990, **74**, 613.

